Chapter 3

Hydraulic Actuation

Hydraulic actuators transform hydraulic power into mechanical power based on Pascal's law, which states that "any change in pressure at any point of an incompressible and confined fluid at rest is transmitted equally in all directions". Even though a fluid is very slightly compressible, this property allows hydraulic actuators to produce large forces and high speeds, becoming thus a very attractive actuation system to dynamic robotic applications.

This section aims to familiarize the robotics community with this kind of actuation, providing insights into the main relevant fluid properties and components, such as pumps, valves and cylinder. Furthermore, the main advantages and drawbacks of this actuation technology are discussed.

Initially, the nonlinear model of the hydraulic actuation employed in HyQ is presented, and afterwards a linearization is carried out for controller design purposes. Despite of all nonlinearities that might be present in hydraulics, a linear model is able to sufficiently describe the hydraulic dynamics. Also, the next chapters will show that simple approaches are sufficient to very effectively control both the position and the force in hydraulic actuators.

3.1 Fluid properties

The most common fluids applied in hydraulic actuation are based on mineral oil. The oil is only very slightly compressible, a fact that makes it very suitable for transmitting power very quickly from one part of the system to the other. Meanwhile, the oil also lubricates and cools down components such as valves and cylinders. HyQ uses the oil-based fluid ISO VG46.

Another fluid that is being focus of research especially in the last decades is the water. Although it is environmentally-friendly, clean, and safe, it is still a challenge to manufacture water-based hydraulic components due to corrosion, flow erosion, and higher internal leakage due to the low water viscosity[Garry W. Krutz, 2004]. A comparison between oil and water hydraulics can be found in [Yang et al., 2009].

The cleanness of the hydraulic fluid is an important issue in hydraulics, and a filter is always necessary. Some components require very low oil contamination levels to work properly. For instance, the HyQ valves [MOOG Inc., 2003], which have a tiny hydraulically driven stage, need a $3\mu m$ filter in the line. Particles in the order of tens of micrometers can already totally or partially clog the valve, reducing its performance or even rendering it unusable. Also, many sealing components, especially towards the end of their life-cycle, start to degrade and contaminate the oil. This fact augments the need of a good filtering system on a hydraulic circuit.

Another important issue in a hydraulic circuit is the temperature. The oil viscosity is highly dependent on its temperature: the viscosity drops when the temperature increases, and vice-versa. The viscosity has a big impact in the fluid dynamics, influencing the response characteristic of closed control loops, as well as its damping and also stability [Merritt, 1967]. To avoid changes in the system performance due to changes in the oil viscosity, the system should operate always around the same temperature. Thus, a cooler is usually installed in the hydraulic circuit to keep the oil in a steady-state temperature. For HyQ, the cooler kicks in when the oil reaches about $40°C$. The cooler is also a safety component, avoiding that the oil heats up too much so that it could damage components, and, in an extreme case, burn people.

3.1.1 Bulk Modulus

The most important fluid property for compliance control is its compressibility. The fluid compressibility is defined by its modulus of elasticity, the so-called *Bulk modulus* β, as follows:

$$\beta = -v_0 \left(\frac{\partial p}{\partial v} \right) \tag{3.1}$$

where,

v_0: initial volume of the confined fluid $[m^3]$

v: final volume of the pressurized fluid $[m^3]$

p: pressure applied to the fluid $[Pa]$

For mineral oil, typical bulk modulus values range from 1400 to 1600 MPa. However, from a practical point of view, this might be a rough approximation, as the bulk modulus varies considerably with pressure, enclosed air, and pipe line compliance. An *effective Bulk modulus* β_e, which takes into account these effects, can be theoretically or empirically estimated. According to Eggerth's method [Jelali and Kroll, 2003], the effective Bulk modulus for HyQ was estimated to be $\beta_e = 1300$ MPa.

3.2 Pump

In hydraulics, the pump is the element that converts mechanical power into hydraulic power. It introduces power into the system by drawing fluid from a reservoir and releasing it with a certain pressure and flow into the output line. In hydraulics, non-SI units are still very often used to describe some physical quantities such as flow (l/min instead of the SI m^3/s) and pressure (bar instead of Pa). Using these commonly used units, the hydraulic power can be mathematically defined as:

$$p_{hyd} = \frac{q\ p}{600} \tag{3.2}$$

where,

p_{hyd}: hydraulic power $[kW]$

q: flow $[l/min]$

p: pressure $[bar]$

The most common sources of power to hydraulic pumps are electric motors and internal combustion engines. The former is usually used in indoor applications, since it is less noisy and it does not expel gases, and the latter in outdoor applications or where energy density is very critical.

Although combustion engines are about 3 times less efficient than electric motors, the energy density of fossil fuels is around 30 times higher than the energy density of the newest commercially available batteries (see Table 3.1). Therefore, many of the robots that are supposed to present a high level of energy autonomy use combustion engine.

	Efficiency	**Energy density**	**Autonomy**
Combustion Engine & Gasoline	30%	12 kWh/kg	40 min/kg
Electric Motor & Battery	90%	0.4 kWh/kg	4 min/kg

Table 3.1: Comparison between two different ways of driving a pump: a *combustion engine* with gasoline as fuel vs. an *electric motor* powered by high-energy batteries. The average efficiency of the actuators, the energy density of the fuel and battery, and the HyQ autonomy considering 1 kg of fuel/battery during a medium-velocity walking (5 kW/h energy consumption) are displayed for each actuation modality. To calculate it, the pump efficiency was considered to be 90% for both cases. The higher autonomy reached with an internal combustion engine is the reason for its use in autonomous hydraulic robots.

There are two main ways of transmitting the hydraulic power from the pump to the actuators. The first way is to use servovalves between the pump and the actuator to control the inlet actuator flow. These systems are called *valve-controlled* systems, and it is also employed in HyQ. The second is to connect the pump directly to the actuator. In this case, the inlet actuator flow is controlled by the speed of the pump. These systems are called *pump-controlled* systems, or also hydrostatic transmissions [Korn and of Technology, 1969]. The faster control capability of valve-controlled systems (servovalves have normally higher bandwidth than pumps) make this arrangement preferred in the majority of applications, including robotics, in spite of its lower theoretical maximum operating efficiency of 67% [Merritt, 1967]. Nevertheless, pump-controlled systems are more efficient and it can be an option for high-power applications that do not require fast responses.

Hydraulic pumps can be divided essentially into two big groups according to their pumping principle. Some pumps carry a fixed amount of fluid volume in every revolution, and they are named *fixed-displacement* or simply *gear pumps* (Fig. 3.1). These pumps always maintain the same outlet flow and a relief valve controls the

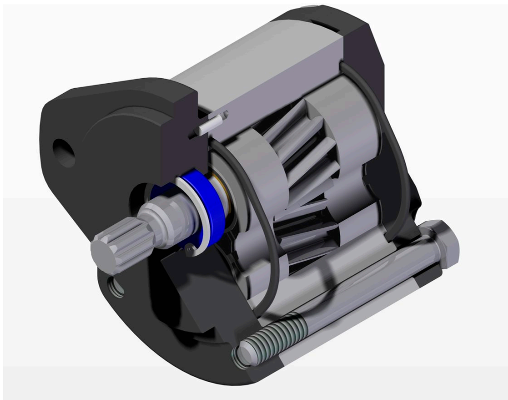

Figure 3.1: CAD picture of a fixed displacement gear pump. It has helical gears, which reduces the backlash (T3S model, from JIHOSTROJ a.s.)

pressure. Thus, if the hydraulic system does not use all of the flow, the remaining flow is returned to the tank through the relief valve. This represents a large loss of power which compromises the efficiency of the overall valve-controlled hydraulic system. On the other hand, *variable-displacement* pumps deliver a variable flow, which changes according to the system demand. This increases significantly the efficiency of a valve-controlled hydraulic circuit. Hence, in autonomous hydraulically-actuated robots that are valve-controlled, a variable-displacement pump should always be preferred to increase the robot efficiency and autonomy.

The main sources of losses of power in hydraulic pumps are friction and internal leakage. The efficiency of pumps can be very dependent on the system pressure: the higher the pressure, the higher the leakage flows and the lower the efficiency. For variable displacement pumps, at low pressures (< 100 *bar*), the pump efficiency can reach 99%, and for higher pressures (< 250 *bar*) the efficiency can drop to about 90%. Also the fluid temperature influences the pump efficiency since the temperature changes the viscosity, and consequently the (leakage) flow dynamics.

3.3 Valve

The valve is the hydraulic component in charge of controlling the hydraulic power, supplied by the pump, that goes to the actuators. The most common type of valve employed on hydraulically-actuated robots, including HyQ, are flow-control servovalves. These valves regulate the output flow according to a control signal input.

HyQ uses off-the-shelf servovalves manufactured by Moog Inc. [MOOG Inc., 2003] (Fig. 3.2a). These valves have four ports (a, b, s, and t) and the valve spool is hydraulically-driven by a pilot stage. The port a connects the valve to the actuator chamber a and the port b to the chamber b, while the port s (stands for Supply) connects the valve to the pump and the port t (stands for Tank) connects the valve to the reservoir. The pressure at the valve ports a, b, s, and t are named as p_a, p_b, p_s, and p_t respectively. The valve input voltage is u. A hydraulic schematic for the valve is depicted in Fig. 3.2b

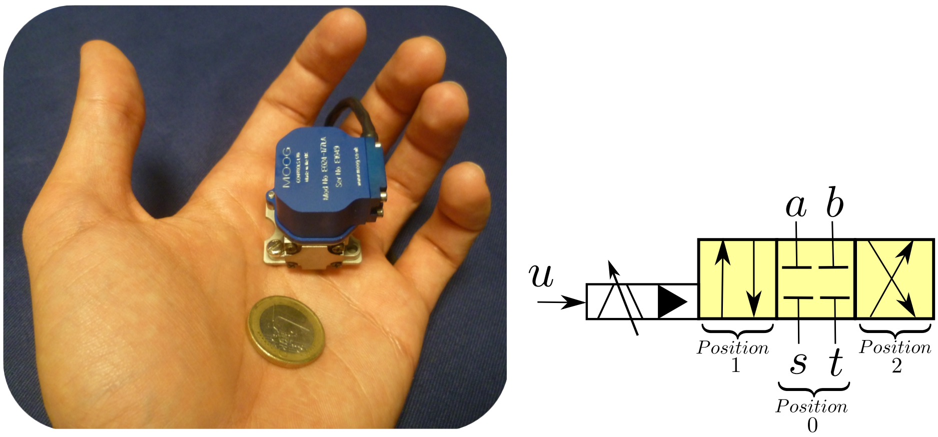

(a) Miniature MOOG E024 servovalves.. **(b)** ..and respective schematic

Figure 3.2: As seen in (a), compared to most of the available servovalves, the HyQ servovalves are small-size and light-weight. The valve schematic in (b) shows the three valve positions and its four ports a, b, s, and t.

In comparison with the commonly available servovalves, these miniature valves have many aspects that make them very suitable for robotics, such as:

- Very compact and light-weight (92 $grams$);
- High bandwidth ($\geq 250\ Hz$);
- High peak flow capability ($7.5\ l/min$)

In the next sections, the main aspects regarding the valve modeling are discussed. Firstly, the valve spool dynamics is presented and, later, the flow equation and parameters are characterized.

3.3.1 Valve spool dynamics

In a servovalve, the spool is a movable part located inside the valve housing. By sliding back and forth it can, totally or partially, block and/or open the valve channels, setting like this the flow direction and magnitude.

The spool moves inside the valve housing according to the electrical input u applied to the valve. The relation between the valve input u and the spool position x_v can be modeled as a linear second order system:

$$\varDelta x_v(s) = \frac{K_{spool}}{\frac{1}{\omega_v^2}s^2 + \frac{2D_v}{\omega_v}s + 1}\varDelta u(s) \tag{3.3}$$

where,

K_{spool}: steady-state valve input-to-spool-position gain $[m/A]$
ω_v: valve spool angular frequency $[rad/s]$
D_v: valve spool damping

The gain K_{spool} relates the input, which for HyQ is a current, to the position of the spool in steady-state. The valve spool natural frequency F_v, where $F_v = \omega_v/2\pi$, is the most important parameter on the valve spool dynamics, and it can be approximated as the *valve bandwidth* [Merritt, 1967]. Essentially, F_v indicates how fast the spool can move. Also, since in the HyQ valves the spool is moved by a hydraulic-pilot stage, F_v is highly dependent on the supply pressure level: *the higher the supply pressure, the higher the valve bandwidth*. For instance, at the maximum supply pressure of 210 bar, F_v is about 250 Hz for $\pm25\%$ of the spool displacement, and about 100 Hz for $\pm100\%$. This high valve bandwidth is a key aspect for reaching high-performance torque and compliance control with hydraulic actuators. This important issue is discussed in more details in Chapters 5 and 6.

The hydraulic pressure and force dynamics are very fast and require a rapid actuation to control them. Therefore, attention must be paid in all the hardware levels to avoid inserting a slower element which could compromise the overall actuation bandwidth by adding delays to the response. For instance, the valve drivers, which usually convert voltage to current or *vice-versa*, must have a fast electrical dynamics so that it does not modify significantly the input from the controller to the valve.

For most of the commercially available servovalves, the spool position cannot be measured. Moreover, usually there is a lack of mechanical details about the valve internal parts on the valve data sheet, so that it might be hard to define gains such as K_{spool}. To overcome these issues, it is useful to express the spool position in terms of the valve input u, that is:

$$\Delta u_v(s) = \frac{1}{\frac{1}{\omega_v^2}s^2 + \frac{2D_v}{\omega_v}s + 1}\Delta u(s) = \frac{1}{K_{spool}}\Delta x_v(s) \tag{3.4}$$

In the above definition, the u_v transfer function has unity gain in steady-state, and u_v has the same units of u, that for the HyQ valve is *Ampere*. Thus, u_v can be seen as a filtered version of the input u, where the lag introduced by the filter corresponds to the spool dynamics delay. In other words, u_v is a current that represents the actual spool position, as if it was the output of a spool position sensor. From here onwards, u_v will refer to the spool position, and x_v will not be used in the modeling.

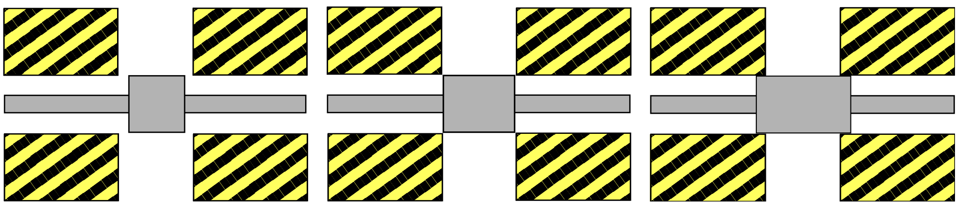

(a) Under-lapped spool **(b)** Zero-lapped spool **(c)** Over-lapped spool

Figure 3.3: Different sizes of spool. In (a) the under-lapped spool land does not cover the whole port orifice and a large internal leakage is observed; in (b) the spool land aligns with the edge of the ports. This is the spool size of the valves used in HyQ; in (c) the spool is over-sized with respect to the valve ports and a dead-band is present around the null spool position.

3.3.2 Flow through valves

As discussed previously, the valve spool is the component in charge of controlling the flow direction and magnitude. The flow magnitude is controlled by manipulating the adjustable area $a(u_v)$ of the valve control orifices, which changes linearly with the spool position u_v, that is:

$$a(u_v) = Wu_v \tag{3.5}$$

where,

W: area gradient $[m^2/A]$

Besides the orifice area $a(u_v)$, the flow magnitude q through an orifice is also a function of the differential pressure Δp across the orifice, and it can be written in the following ways:

$$q = C_d a(u_v)\sqrt{\frac{2\Delta p}{\rho}} = C_d W u_v \sqrt{\frac{2\Delta p}{\rho}} = \frac{C_d W\sqrt{2}}{\sqrt{\rho}} u_v \sqrt{\Delta p} = K_v u_v \sqrt{\Delta p} \tag{3.6}$$

where,

C_d: discharge coefficient ($C_d \approx 0.6$ is often assumed [Merritt, 1967])

ρ: oil density (for HyQ ISO VG46 oil, $\rho = 850\ kg/m^3$)

K_v: valve gain

As seen in the right-side of Eq. 3.6, the term that multiplies $u_v\sqrt{\Delta p}$ can be written as a constant K_v and it accounts essentially for the valve size. Again, due to the lack of information in most valve data sheets, it might be difficult to estimate W and also to obtain a precise equation for the flow. Thus, another definition for this sizing constant, which is based on common data sheet information, is presented [De Negri et al., 2008].

3.3.2.1 Valve gain

Usually, the way valve manufacturers give information about the valve size in the data sheets is through three parameters: *nominal flow*, *nominal pressure drop*, and *nominal valve input*. In many cases, the nominal points are given as the maximum ones, however any operating point within the valve flow range can be used for sizing it.

The standard procedure for obtaining these three nominal parameters is by interconnecting the valve control ports a and b ($p_a = p_b$), applying a constant electrical input u_{vn} to the valve, and measuring the steady-state flow q_n which passes through the valve.

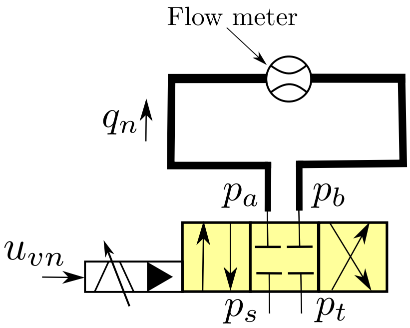

Figure 3.4: Hydraulic circuit schematic for determining the valve gain

Assuming the pressure drop Δp_{n1} across the ports s and a is the same as across the ports b and t ($\Delta p_{n1} = p_s - p_a = p_b - p_t$), the nominal pressure drop across all the valve control ports can be written as:

$$\Delta p_{n2} = (p_s - p_a) + (p_b - p_t) = p_s - p_t = 2\Delta p_{n1} \tag{3.7}$$

where,

Δp_{n1}: nominal pressure drop across one control port of the valve $[Pa]$

Δp_{n2}: nominal pressure drop across two control ports of the valve $[Pa]$

It is important to identify in the valve data sheet which pressure drop is given, whether it is across one or two control ports, to be able to properly estimate the valve size. The most common pressure drop to be reported in data sheets is Δp_{n2}.

Once the nominal flow with the respective pressure drop and valve input are known, Eq. 3.6 can be rewritten for the nominal case and the valve gain K_v can be redefined as:

$$K_v = \frac{c_d W \sqrt{2}}{\sqrt{\rho}} = \frac{q_n}{u_{vn}\sqrt{\Delta p_{n1}}} = \frac{q_n}{u_{vn}\sqrt{\frac{\Delta p_{n2}}{2}}} \tag{3.8}$$

where,

u_{vn}: nominal valve input $[A]$

q_n: nominal flow $[m^3/s]$

The definition of the valve sizing gain K_v shown in Eq. 3.8 is very easily obtainable from the valve datasheet. Therefore, from here onwards the flow equation will always be written in terms of K_v.

3.4 Asymmetric Cylinder

The most common actuator in hydraulics is the linear actuator, or hydraulic cylinder. It converts hydraulic energy into mechanical energy. It consists of two main parts: a hollow cylindrical body and a piston, which is inserted inside the body and is free to move. The piston rod is the part which connects the piston to an external object, or more generically, to a load.

There are essentially two kind of cylinders: cylinders with rods at both extremities (named symmetric or double-rod cylinders) and cylinders with only one rod (called asymmetric or single-rod cylinders), as depicted in Fig. 3.5a.

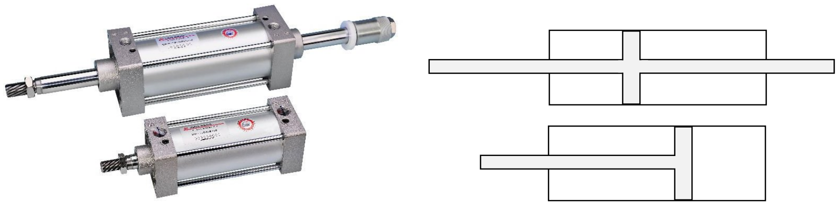

(a) **(b)**

Figure 3.5: (a): Picture of symmetric and asymmetric cylinders; and (b) the respective hydraulic schematic used to represent these components.

As mentioned before, HyQ uses asymmetric cylinders for moving the HFE and KFE joints (see Fig. 1.2a and Fig. 1.2b). In these kind of cylinders, the asymmetry leads to different effective chamber areas. The larger area A_p is called piston area. The rod-side area, also called annular area, is smaller by a factor of $\alpha < 1$. Symmetric cylinders have $\alpha = 1$. For the HyQ cylinders, this area ratio is $\alpha \cong 0.61$.

The hydraulic schematic shown in Fig. 3.6 represents the hydraulic actuation circuit that is employed in the hydraulically-actuated joints of HyQ. It is composed of a servovalve and an asymmetric cylinder. The inertial load is represented by a mass M_l with viscous friction B_l, which includes mainly the friction in the joint

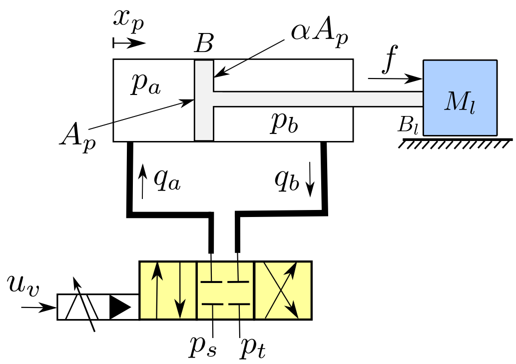

Figure 3.6: Hydraulic schematic of the HyQ hydraulic actuation system. The valve, in yellow, choses the direction and magnitude of the chamber flows q_a and q_b. These flows change the pressures p_a and p_b inside the asymmetric cylinder chambers, and consequently the force f that is transmitted to the load, which takes into account the cylinder friction B. The load, represented by the blue block, is simplified in this schematic to be an inertial load with constant mass M_l and friction B_l.

bearings. Throughout this thesis, the color blue will always be associated to the load, and the yellow color to the actuation.

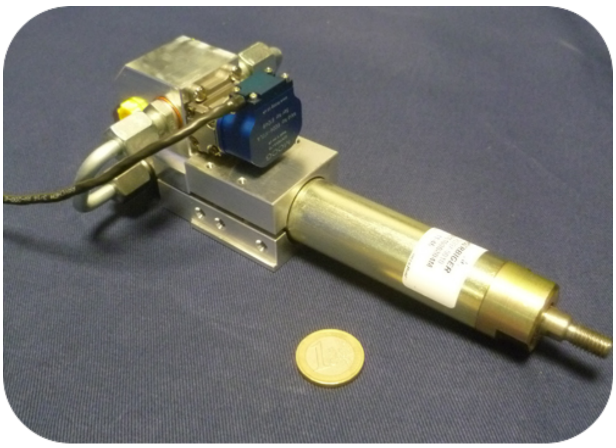

Figure 3.7: The HyQ valves are attached as close as possible to the cylinder to reduce the hydraulic compliance of the system. Also, rigid tubes are used to connect both. These two design decisions increase the actuation bandwidth.

The HyQ valves are assembled on a small manifold which is mounted directly on the cylinder body. The valve ports a and b are connected to the cylinder ports through rigid tubes in an “u” shape, as depicted in Fig. 3.7. To place the valves as close as possible to the cylinder has the main goal of reducing the compliance of the system. This reduction is achieved by reducing the amount of oil between the valve and the cylinder and also by using rigid tubes instead of flexible hoses. This topic is further discussed in Chapter 7.

The chamber flows q_a and q_b can be modeled as Eq. 3.6, depending on the valve spool position u_v:

$$q_a = \begin{cases} K_v u_v \sqrt{p_s - p_a}, & u_v > 0. \\ K_v u_v \sqrt{p_a - p_t}, & u_v < 0. \end{cases} \tag{3.9}$$

$$q_b = \begin{cases} K_v u_v \sqrt{p_b - p_t}, & u_v > 0. \\ K_v u_v \sqrt{p_s - p_b}, & u_v < 0. \end{cases} \tag{3.10}$$

Neglecting external and internal leakages, the mass conservation principle can be applied to each of the chambers by using the continuity equation, and the following well-known expressions for the chamber pressure dynamics can be written [Merritt, 1967]:

$$\dot{p_a} = \frac{\beta_e}{v_a}\left(q_a - A_p \dot{x}_p\right) \tag{3.11}$$

$$\dot{p_b} = \frac{\beta_e}{v_b}\left(-q_b + \alpha A_p \dot{x}_p\right) \tag{3.12}$$

where,

v_a: chamber a volume $[m^3]$

v_b: chamber b volume $[m^3]$

The chamber volumes vary according to the piston position x_p. The volume inside the hoses which connect the valve to the actuator is also included in the total volumes chamber, which can be defined as follows:

$$v_a = V_{pl} + A_p x_p \tag{3.13}$$

$$v_b = V_{pl} + (L_c - x_p)\alpha A_p \tag{3.14}$$

where,

V_{pl}: pipe line volume $[m^3]$

L_c: cylinder length or stroke (total distance the cylinder can travel) $[m]$

The pipe line volume V_{pl} depends on the internal diameter D_{pl} of the pipe and on its length L_{pl} ($V_{pl} = L_{pl}\pi D_{pl}^2/4$).

3.4.1 Hydraulic Force

The hydraulic force f_h created by the hydraulic cylinder is defined as the force created exclusively by the difference of pressures in the cylinder chambers, that is:

$$f_h = A_p p_a - \alpha A_p p_b = A_p(p_a - \alpha p_b) \tag{3.15}$$

The pressure difference $p_a - \alpha p_b$ can also be defined as the *load pressure* for an asymmetric cylinder. It is the pressure difference that effectively produces a force. Thus, Eq. 3.15 can be rewritten as:

$$f_h = A_p p_l \tag{3.16}$$

where,
p_l: load pressure ($p_l = p_a - \alpha p_b$) $[Pa]$

Taking the time derivative of Eq. 3.15, and considering the definition of load pressure as well as Eq. 3.11 and 3.12, the hydraulic force dynamics can be obtained as follows:

$$\dot{f}_h = \frac{A_p\beta_e}{v_a}(q_a - A_p\dot{x}_p) - \frac{\alpha A_p\beta_e}{v_b}(-q_b + \alpha A_p\dot{x}_p) \tag{3.17}$$

3.4.2 Friction Force

Since hydraulic components such as cylinders are used to work with fluids under high pressures, the piston sealing is usually quite tight to avoid internal leakages. This small clearance in between the cylinder piston and the cylinder body increases substantially the friction forces, which work also as natural damping, but also insert nonlineartities into the system.

The friction forces in a hydraulic cylinder can be modeled as follows [Jelali and Kroll, 2003]:

$$f_f = B\dot{x}_p + sign(\dot{x}_p)\left(F_{c_0} + F_{s_0}\, e^{-\frac{|\dot{x}_p|}{C_s}}\right) \tag{3.18}$$

where,

B: viscous friction coefficient $[Ns/m]$

F_{c_0}: Coulomb friction coefficient $[N]$

F_{s_0}: static friction coefficient $[N]$

C_s: static decay friction coefficient (known also as Stribeck velocity) $[m/s]$

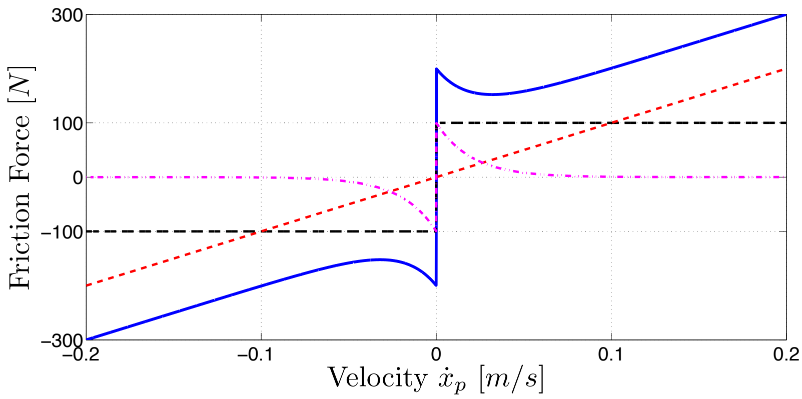

Figure 3.8: Typical theoretical friction curve for a hydraulic actuator. The continuous blue line shows the total friction force f_f, and it is the sum of all the other three curves. The black dashed line plots the constant Coulomb friction for $F_{c_0} = 100\ N$; the pink dot-dashed line the static friction with $F_{s_0} = 100\ N$ and $C_s = 0.02$; and the red dashed line the linear viscous friction considering $B = 1000\ Ns/m$.

As seen in Eq. 3.18 and Fig. 3.8, the friction forces in hydraulic cylinders can be decomposed essentially in three main components:

- Viscous friction: it is the only linear component of the friction forces, and because of that it is usually the only force considered in the modeling. It is proportional to the piston velocity magnitude.

- Coulomb friction: it is a constant force that depends only on the sign of the piston velocity.

- Static friction: this force acts mainly at zero velocity. It decays exponentially to zero as soon as the piston starts to move.

All these parts create the well-known Stribeck forces curve, shown in Fig. 3.8 [Armstrong-Hélouvry et al., 1994]. For HyQ, the friction forces f_f were estimated experimentally by measuring the hydraulic force f_h with pressure sensors, and also the load force f with a load cell, as shown in Eq. 3.19. The results were very dependent on the system velocity. As seen in Fig. 3.9a, 3.9b, and 3.9c, a hysteresis nonlinearity was always present, especially for positive velocities. At low velocities the curve was more linear, being the Coulomb friction estimated as $F_{c_0} \cong 100\ N$. The viscous friction coefficient was estimated as $B \cong 1000\ Ns/m$. Some models that describe the nonlinearities seen in these experimental data can be found in the literature [Xuan Bo Tran and Yanada., 2012].

The high friction in hydraulic actuators is a drawback from the energy point of view. A significant part of the fluid power is lost in friction. However, this high friction is also beneficial for the force controller. It essentially increases the stability margins. The higher the friction, the faster the hydraulic force controller can respond. This topic is further discussed in Section 7.1.2.

3.4.3 Load force

The force that is truly applied to a load attached to the piston rod is called herein *load force*, and it is defined as the difference between the hydraulic force f_h produced by the load pressure and the forces f_f lost through friction, that is:

$$f = f_h - f_f \tag{3.19}$$

where,

f: load force $[N]$

In the HyQ leg, the load force is measured by a small-size load cell attached in series with the piston rod (Fig. 3.10b). As it is described in Chapter 5, this measurement is used to control the torque that is applied to the joints of HyQ, and also to control its compliance.

The miniature load cell, shown in Fig. 3.10a has an axial force measurement range of 10000 N ($-5000\ N$ to $5000\ N$). This large range is required to guarantee mechanical robustness and control accuracy even in presence of the big impacts that

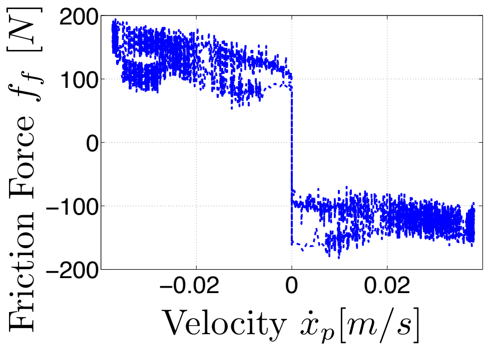

(a) 0.1 Hz

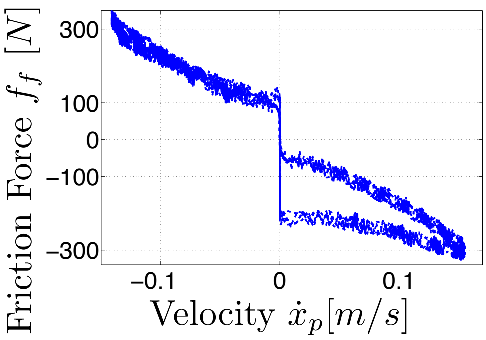

(b) 1 Hz

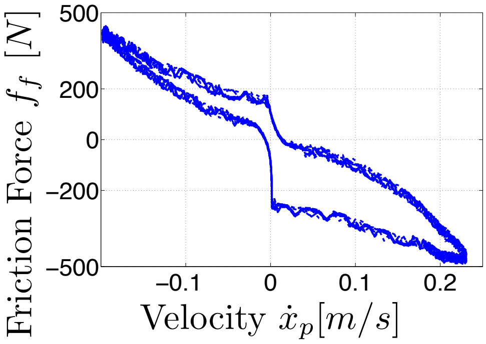

(c) 3 Hz

Figure 3.9: Friction forces obtained with the HyQ cylinder for different velocity ranges. A sinusoidal motion was applied to the piston at different frequencies. As seen, many nonlinearities are present in the response. For a low speed experiment shown in (a), the viscous friction coefficient was estimated as $B \cong 1000$ Ns/m while the Coulomb friction as $F_{c_0} \cong 100$ N.

(a) (b)

Figure 3.10: The HyQ load cell, shown in (a), is able to measure axial forces in the range of $-5000\ N$ to $5000\ N$. In (b), the HyQ cylinder is connected with the load cell in series with the rod.

the HyQ leg can face during locomotion tasks. It has a relatively small noise of $\pm 1\%$ in comparison with the whole range. However, in absolute values it is relatively high ($\pm 50\ N$). This noise degrades the force control performance when it has to control forces that are in the range of the noise. Strong filtering cannot be used because it would introduce significant delays into the fast force dynamics and reduce the overall system stability. This issue is further discussed in Section 6.2.

The load force dynamics can be expressed by taking the time derivative of Eq. 3.19. Taking into account Eq. 3.9, 3.10, and 3.17, and considering only the viscous friction, the following load force dynamics can be written:

$$\dot{f} = \dot{f}_h - B\ddot{x}_p =$$
$$= \begin{cases} -\beta_e A_p^2 \left(\frac{1}{v_a} + \frac{\alpha^2}{v_b}\right)\dot{x}_p - B\ddot{x}_p + \beta_e A_p K_v \left(\frac{\sqrt{p_s - p_a}}{v_a} + \frac{\alpha\sqrt{p_b - p_t}}{v_b}\right) u_v, & u_v > 0. \\ -\beta_e A_p^2 \left(\frac{1}{v_a} + \frac{\alpha^2}{v_b}\right)\dot{x}_p - B\ddot{x}_p + \beta_e A_p K_v \left(\frac{\sqrt{p_a - p_t}}{v_a} + \frac{\alpha\sqrt{p_s - p_b}}{v_b}\right) u_v, & u_v < 0. \end{cases} \tag{3.20}$$

The load force dynamics equation shown in Eq. 3.20 might be the most important equation in this chapter. The force model-based controllers, described in Chapter 5, are based on this equation.

3.5 Hydraulic actuation linearized model

A linear model can be very useful for understanding the system characteristics through the use of linear system's tools, such as transfer functions, root locus, and bode plot. These tools also help in designing simple linear controllers, such as the well-known PID controller.

In this section, the nonlinear model described in the previous section will be linearized around an operating point $P_{\oslash} = (p_{a\oslash}, p_{b\oslash}, u_{v\oslash})$. The most common operating point used in the literature to linearize the nonlinear hydraulic dynamics is $P_{\oslash} = (\frac{p_s}{2}, \frac{p_s}{2}, 0)$ [Jelali and Kroll, 2003]. The operating pressures $p_{a\oslash}$ and $p_{b\oslash}$, in this case, are the same and maintain a symmetric cylinder in equilibrium, that is, with load pressure $p_{l\oslash} = 0$.

For an asymmetric cylinder, for achieving a force equilibrium the operating pressures cannot be the same since the effective piston areas are different. Thus, a more convenient operating point can be defined as $P_{\oslash} = (\frac{\alpha p_s}{1+\alpha}, \frac{p_s}{1+\alpha}, 0)$. With these new pressures $p_{a\oslash}$ and $p_{b\oslash}$, the load pressure $p_{l\oslash}$ for an asymmetric cylinder is zero and the cylinder is in equilibrium. For $\alpha = 1$ (symmetric cylinder) the previous operating point $P_{\oslash}$ is obtained.

Regarding the operating valve spool position, $u_{v\oslash} = 0$ is normally chosen since most of the valves have symmetric opening and the spool is mainly moving around this null position.

In the next sections, the nonlinear flow and pressure dynamics will be linearized around this equilibrium point $P_{\oslash}$ to obtain a linear load force dynamics.

3.5.1 Valve coefficients

The chamber flows dynamics, described in Eq. 3.9 and 3.10, are nonlinear. To linearize them, they can be expanded using Taylor series about the equilibrium point $P_{\oslash}$ and truncated after the first differential term [Merritt, 1967]:

$$\Delta q_a = K_{qa} \Delta u_v - K_{ca} \Delta p_a \tag{3.21}$$

$$\Delta q_b = K_{qb} \Delta u_v - K_{cb} \Delta p_b \tag{3.22}$$

The terms K_{qa}, K_{qb}, K_{ca}, and K_{cb} are part of the so-called *valve coefficients*. These coefficients represent the main characteristics of a valve, and they can be defined as:

$$K_{qa} = \left.\frac{\partial q_a}{\partial u_v}\right|_{P_\oslash} = \begin{cases} K_v\sqrt{p_s - p_{a\oslash}}, & u_v > 0. \\ K_v\sqrt{p_{a\oslash} - p_t}, & u_v < 0. \end{cases} \tag{3.23}$$

$$K_{qb} = \left.\frac{\partial q_b}{\partial u_v}\right|_{P_\oslash} = \begin{cases} K_v\sqrt{p_{b\oslash} - p_t}, & u_v > 0. \\ K_v\sqrt{p_s - p_{b\oslash}}, & u_v < 0. \end{cases} \tag{3.24}$$

$$K_{ca} = -\left.\frac{\partial q_a}{\partial p_a}\right|_{P_\oslash} = \begin{cases} \frac{K_v u_{v\oslash}}{2\sqrt{p_s - p_{a\oslash}}}, & u_v > 0. \\ \frac{-K_v u_{v\oslash}}{2\sqrt{p_{a\oslash} - p_t}}, & u_v < 0. \end{cases} \tag{3.25}$$

$$K_{cb} = -\left.\frac{\partial q_b}{\partial p_b}\right|_{P_\oslash} = \begin{cases} \frac{-K_v u_{v\oslash}}{2\sqrt{p_{b\oslash} - p_t}}, & u_v > 0. \\ \frac{K_v u_{v\oslash}}{2\sqrt{p_s - p_{b\oslash}}}, & u_v < 0. \end{cases} \tag{3.26}$$

K_{qa} and K_{qb} are called *flow gains*. They describe how much flow is produced for a certain valve opening. They also directly affect the open-loop gain in a system and therefore its stability. The *flow-pressure coefficients* K_{ca} and K_{cb} characterize the leakage in the valve, that is, how the flow is influenced by a change in pressure. They directly affect the damping of the valve-actuator combination [Merritt, 1967].

Another important valve characteristic is the *pressure sensitivity*, which is defined by:

$$K_{pa} = \left.\frac{\partial p_a}{\partial u_v}\right|_{P_\oslash} = \frac{K_{qa}}{K_{ca}} \begin{cases} \frac{2K_v(p_s - p_{a\oslash})}{u_{v\oslash}} & u_v > 0. \\ \frac{-2K_v(p_{a\oslash} - p_t)}{u_{v\oslash}}, & u_v < 0. \end{cases} \tag{3.27}$$

$$K_{pb} = \left.\frac{\partial p_b}{\partial u_v}\right|_{P_\oslash} = \frac{K_{qb}}{K_{cb}} \begin{cases} \frac{-2K_v(p_{b\oslash} - p_t)}{u_{v\oslash}} & u_v > 0. \\ \frac{2K_v(p_s - p_{b\oslash})}{u_{v\oslash}}, & u_v < 0. \end{cases} \tag{3.28}$$

As seen in Eq. 3.25 and 3.26, and Eq. 3.27 and 3.28, for an ideal valve at the null position ($u_{v\oslash} = 0$) the flow-pressure coefficients are theoretically zero ($K_{ca} = K_{cb} = 0$) and the pressure sensitivities are infinity ($K_{pa} = K_{pb} = \infty$). Nevertheless, more realistic values can be obtained through experimental tests with the valve to increase the fidelity of the model. For instance, in Fig. 3.11b the pressure sensitivities for the HyQ valves can be estimated through the slope of the pressure curves as $K_{pa} \cong K_{pb} \cong 5.7 \cdot 10^{11}$ $[Pa/A]$.

The hydraulic circuit used to obtain the pressure sensitivities are depicted in Fig. 3.11a. In this circuit, the valve ports are blocked, a slow sinusoidal input u

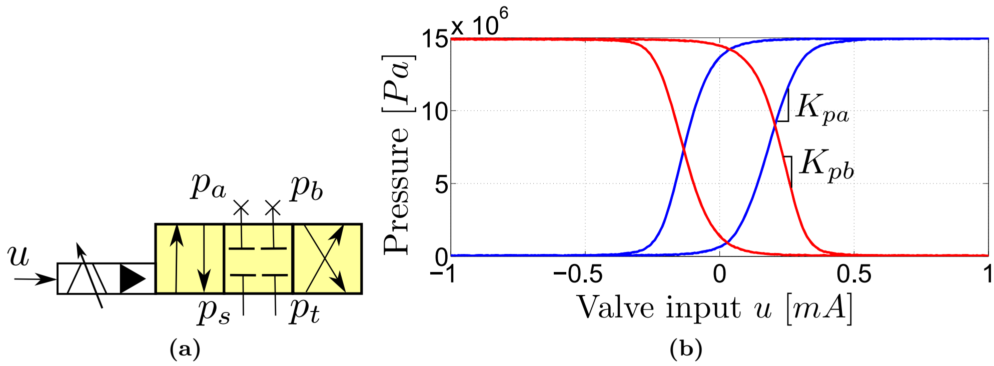

Figure 3.11: (a): Hydraulic schematic of the hydraulic circuit used for obtaining the pressure sensitivity coefficient. The valve ports a and b are blocked and a very slow sinusoidal input u is applied to the valve. The results are shown in (b), where the valve pressure sensitivity coefficients can be estimated as the slope of the pressure curves. The pressure p_a is displayed in blue and p_b in red.

is applied to the valve, and the pressures p_a and p_b are measured using pressure sensors.

The HyQ valve flow gain is presented in the valve datasheet. Thus, an experimental test to identify them was not necessary.

3.5.2 Steady-state and constant volume constraints

The most common linear model found in the literature for describing the force dynamics produced by a hydraulic cylinder is based on the following well-known steady-state flow relations:

$$q_a = A_p \dot{x}_p \tag{3.29}$$

$$q_b = \alpha A_p \dot{x}_p \tag{3.30}$$

Combining these steady-state equations with Eq. 3.9 and 3.10, and assuming p_s and p_t constant, the pressures p_a and p_b can be linearized as a function of the load pressure p_l as:

$$\Delta p_a = \frac{1}{1+\alpha^3} \Delta p_l \tag{3.31}$$

$$\varDelta p_b = \frac{-\alpha^2}{1+\alpha^3}\varDelta p_l \tag{3.32}$$

Another common simplification done in the literature during linearization is to assume that the cylinder volumes v_a and v_b are constant. This is a valid assumption if the piston velocity $\dot{x}_{p\oslash}$ and valve opening $u_{v\oslash}$ at the operating point are both zero.

Thus, considering v_a and v_b constant, the hydraulic force (Eq. 3.17) can be linearized as:

$$\begin{aligned} \varDelta \dot{f}_h = \left.\frac{\partial \dot{f}_h}{\partial q_a}\right|_{P_\oslash} \varDelta q_a + \left.\frac{\partial \dot{f}_h}{\partial q_b}\right|_{P_\oslash} \varDelta q_b + \left.\frac{\partial \dot{f}_h}{\partial \dot{x}_p}\right|_{P_\oslash} \varDelta \dot{x}_p = \\ \frac{A_p\beta_e}{v_{a\oslash}}\left(\varDelta q_a - A_p\varDelta \dot{x}_p\right) - \frac{\alpha A_p \beta_e}{v_{b\oslash}}\left(-\varDelta q_b + \alpha A_p \varDelta \dot{x}_p\right) \end{aligned} \tag{3.33}$$

where,

$v_{a\oslash}$: volume of the chamber a at the operating point $[m^3]$

$v_{b\oslash}$: volume of the chamber b at the operating point $[m^3]$

Taking into account the linear relations for the flows (Eq. 3.21 and 3.22) and pressures (Eq. 3.31 and 3.32), the linear hydraulic force dynamics can be written as:

$$\varDelta \dot{f}_h = K_{\dot{x}_p}\varDelta \dot{x}_p + K_{u_v}\varDelta u_v + K_{f_h}\varDelta f_h \tag{3.34}$$

where the linear constants $K_{\dot{x}_p}$, K_{u_v}, and K_{f_h} are defined as:

$$K_{\dot{x}_p} = -A_p^2\beta_e\left(\frac{1}{v_{a\oslash}} + \frac{\alpha^2}{v_{b\oslash}}\right) \tag{3.35}$$

$$K_{u_v} = A_p\beta_e\left(\frac{K_{qa}}{v_{a\oslash}} + \frac{\alpha K_{qb}}{v_{b\oslash}}\right) \tag{3.36}$$

$$K_{f_h} = \frac{\beta_e}{1+\alpha^3}\left(\frac{K_{ca}}{v_{a\oslash}} - \frac{\alpha^3 K_{cb}}{v_{b\oslash}}\right) \tag{3.37}$$

The Laplace transform of Eq. 3.34 can be represented with the block diagram shown in Fig. 3.12. The inertial load has mass M_l. The cylinder friction B was

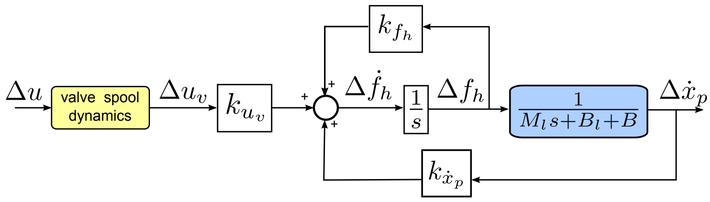

Figure 3.12: Block diagram of the hydraulic force dynamics. The load, represented by the blue block, was modeled as a constant mass M_l. The cylinder friction B was added to the load friction B_l since the rod can be considered part of the load when a hydraulic force f_h is applied.

added to the load damping B_l. As it is shown in Chapter 7, this load damping B_l cannot be neglected in the hydraulic modeling. Also, if the valve spool dynamics shown in Eq. 3.4 is taken into account, the following transfer function can be written:

$$\frac{\Delta f_h(s)}{\Delta u(s)} = \left(\frac{1}{\frac{1}{\omega_v^2}s^2 + \frac{2D_v}{\omega_v}s + 1}\right)\left(\frac{K_{u_v}(M_l s + B_l + B)}{(s - K_{f_h})(M_l s + B_l + B) - K_{\dot{x}_p}}\right) \tag{3.38}$$

Once the linear hydraulic force dynamics, shown in Eq. 3.34, was obtained, the linear load force dynamics can be finally written using the relation presented in Eq. 3.20, where only the cylinder viscous friction B is considered.

$$\Delta \dot{f} = K_{\dot{x}_p}\Delta \dot{x}_p + K_{u_v}\Delta u_v + K_{f_h}\Delta f_h - B\Delta \ddot{x}_p \tag{3.39}$$

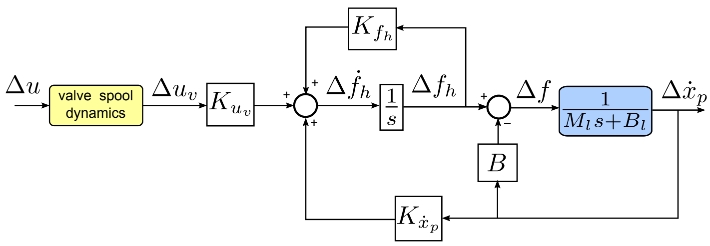

Figure 3.13: Block diagram for the linearized load force

Again, by applying the Laplace transform to Eq. 3.39, the block diagram shown in Fig. 3.13 can be obtained. In this block diagram, the cylinder friction B was separated from the load dynamics. Thus, the load dynamics block depicts only the load friction B_l, which is derived mainly from bearings. Considering the valve spool dynamics, the following transfer function can be written:

$$\frac{\Delta f(s)}{\Delta u(s)} = \left(\frac{1}{\frac{1}{\omega_v^2}s^2 + \frac{2D_v}{\omega_v}s + 1}\right)\left(\frac{K_{u_v}(M_l s + B_l)}{(s - K_{f_h})(M_l s + B_l + B) - K_{\dot{x}_p}}\right) \tag{3.40}$$

The linear hydraulic force Δf_h and the linear load force Δf have very similar dynamics. As seen in Eq. 3.38 and Eq. 3.40, they have exactly the same poles. However, the locations of the zeros are different. The zero from the load force dynamics Δf is closer to the origin then the zero from the hydraulic force dynamics Δf_h, as shown in the root locus in Fig. 3.14b and 3.14a. The high-frequency poles from the valve dynamics are not depicted in these root loci.

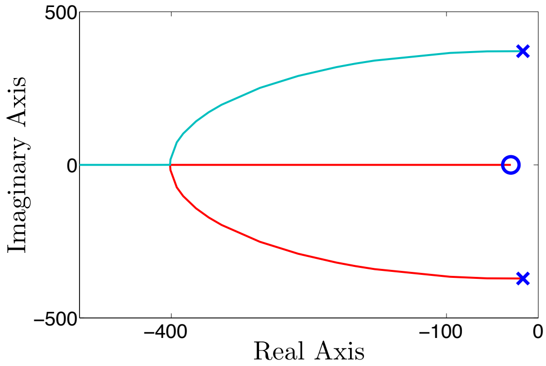

(a) Δf_h root locus

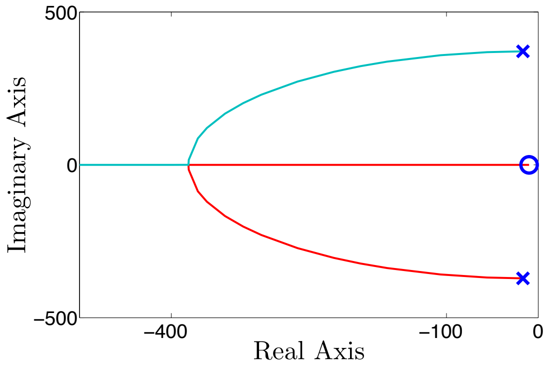

(b) Δf root locus

Figure 3.14: Root locus for the dominant poles of the linear hydraulic ((a)) and load forces ((b)). The poles from the valve dynamics are in high frequencies and are not displayed in this graph. The complex conjugated poles from the load and cylinder/valve dynamics are depicted with blue crosses. As seen in (a), Δf_h has a real zero at around $s = -30\ rad/s$ while Δf in (b) has a zero at $s = -10\ rad/s$. Both are represented by blue circles. This higher frequency zero permits to obtain a faster closed-loop force dynamics with the hydraulic force than with the load force.